Stratospheric CH_3CN from the UARS Microwave Limb Sounder

Nathaniel J. Livesey[1], Joe W. Waters[1], Rashid Khosravi[2], Guy P. Brasseur[3], Geoffrey S. Tyndall[2] and William G. Read[1]

Abstract. CH_3CN in the stratosphere has been measured by the Microwave Limb Sounder (MLS) on the Upper Atmosphere Research Satellite (UARS), providing the first global CH_3CN dataset. The MLS observations are in broad agreement with past high and midlatitude observations of CH_3CN, although concentrations are a little larger than previously observed. In the tropics, where CH_3CN has not up to now been measured, a persistent 'peak' in the profiles is seen around 22 hPa, indicating a possible stratospheric source. Comparisons are made with the NCAR SOCRATES model, including runs having an artificial tropical stratospheric CH_3CN source.

1. Introduction

Methyl cyanide (CH_3CN, also known as acetonitrile) is a comparatively long-lived trace constituent of the Earth's atmosphere. The principal source is biomass burning [*Arijs and Brasseur*, 1986; *Hamm and Warneck*, 1990], which contributes an estimated 0.5–1.0 Tg/year of CH_3CN to the troposphere [*Holzinger et al.*, 1999]. CH_3CN plays an important role in the chemistry of stratospheric ions; it displaces water in ion clusters $H^+(H_2O)_n$, leading to clusters $H^+(CH_3CN)_m(H_2O)_{n-m}$. Detection of these clusters led to the presence of CH_3CN in the stratosphere being deduced and initially quantified (*Böhringer and Arnold* [1981] and references therein). Initial results indicated less than 10 pptv (parts per trillion by volume) of CH_3CN in the stratosphere. Early studies [*Murad et al.*, 1984] suggested that HCN might be a source of stratospheric CH_3CN, but modeling studies [*Brasseur et al.*, 1985] indicated that this is unlikely.

Early observations of tropospheric CH_3CN were somewhat contradictory. Initial gas chromatography measurements indicated a surface mixing ratio of 7 000 pptv. Concentrations as high as 35 000 pptv were observed following a fire in a rural area [*Becker and Ionescu*, 1982]. More recent chromatography measurements at the surface [*Snider and Dawson*, 1984] indicate much lower abundances (56 pptv on average), with observations [*Hamm and Warneck*, 1990] ranging from ∼50 pptv in the middle of the Atlantic to an

[1]Jet Propulsion Laboratory, California Institute of Technology, Pasadena, California.

[2]Atmospheric Chemistry Division, National Center for Atmospheric Research, Boulder, Colorado.

[3]Max Planck Institute for Meteorology, Hamburg, Germany.

average of ∼150 pptv in urban areas, and some urban values as high as 865 pptv. Biomass burning can produce 10^6 pptv CH_3CN [*Lobert et al.*, 1990; *Holzinger et al.*, 1999].

The main chemical loss mechanism for CH_3CN is thought to be reaction with OH [*Arijs and Brasseur*, 1986]. The CH_3CN lifetime from this reaction varies from ∼1 year at the surface to 20 years at 20 km, decreasing to 1 month at 40 km. Reactions with $O(^1D)$, $O(^3P)$ and Cl are thought to be less important, although $O(^3P)$ is significant in the mesosphere. Measurements of *Schneider et al.* [1997] show a decrease in CH_3CN in the lowest 4 km of the stratosphere, indicating a lifetime of ∼1 year; the authors suggest ion-catalyzed destruction as a possible mechanism. The primary sink for tropospheric CH_3CN is thought to be uptake in liquid water (by rain and oceans). A lifetime as short as 15 days due to ocean uptake is possible [*Hamm et al.*, 1984].

2. MLS Measurements of CH_3CN

Figure 1.

MLS is one of ten instruments on UARS, launched in September 1991 [*Waters et al.*, 1999]. MLS observes microwave thermal emission from the Earth's limb. The observations of interest for this study are from bands 2 and 3, where previously identified spectral contributors are ClO, SO_2 and HNO_3. Figure 1 shows spectra for a time and region where the ClO, HNO_3 and SO_2 signals are very weak. These are dominated by a feature near 0.9 GHz intermediate frequency that can be explained by emission from rotational lines of CH_3CN near 202.3 GHz [*Pickett et al.*, 1992]. These lines are relatively strong on a per-molecule basis, because of the large dipole moment (3.9 D) of CH_3CN. The algorithms used to produce MLS data prior to version 5 did not consider CH_3CN emission. This led to some unrealistic biases in other MLS measurements: persistent retrieved SO_2 values of 2 ppbv at 22–10 hPa, long after the decay of the Mt. Pinatubo injected volcanic SO_2, and a negative bias in nighttime ClO at 46 to 4.6 hPa. The version 5 algorithms consider CH_3CN emission and retrieve CH_3CN profiles.

CH_3CN abundances are retrieved on the standard UARS pressure surfaces from 100 to 0.14 hPa at a resolution of six surfaces per decade change in pressure. The CH_3CN data at 100 hPa are unreliable, where the spectral signature is somewhat contaminated by $H_2{}^{18}O$, and are not considered reliable above 1 hPa. The typical precision on a single profile is 40–60 pptv from 68–6.8 hPa; averaging (e.g. zonal mean) is needed to produce results useful for scientific studies.

The absolute accuracy of the CH_3CN observations is estimated at 10 pptv plus 20%. This is based on a 10% uncertainty in the CH_3CN pressure-broadened line width, and an analysis similar to that for UARS MLS ClO observations [*Waters et al.*, 1996]. The vertical resolution, as characterized by the width of the averaging kernels [*Rodgers*, 1990],

is ∼4 km from 68–10 hPa, broadening to 8 km at 1 hPa.

3. Results

Figure 2.

Figure 2 compares MLS CH_3CN results with previous observations. The high latitude MLS data are in reasonable agreement with previous observations in the lower stratosphere, but MLS shows higher abundances in the upper stratosphere. MLS shows CH_3CN to be more abundant in the tropical stratosphere than at higher latitudes.

The NCAR SOCRATES model (Simulation of Chemistry, RAdiation, and Transport of Environmentally important Species) has been used to provide model results for comparison with the MLS data. SOCRATES is a 2-D interactive model that extends from 85°S to 85°N in latitude and from the surface to 120 km in altitude. The horizontal and vertical resolutions are 5° and 1 km, respectively. The model chemistry includes 55 species and 144 gas phase, 5 heterogeneous (PSC/aerosol), and 47 photolysis reactions. The reaction rate coefficients and absorption cross sections are from the JPL 1997 compilation [*DeMore et al.*, 1997]. The model includes all the CH_3CN chemical loss reactions mentioned earlier. Surface boundary conditions are specified as mixing ratios which, based on prior observations of tropospheric CH_3CN, decrease with latitude from 100 pptv at the equator to 20 pptv at the poles.

Figure 2 includes the model CH_3CN results for the latitudes and months of the MLS profiles shown. The model and MLS equatorial results are in good agreement near 25 and 40 km but MLS shows a peak around 33 km that is indicative of a stratospheric source. The model has no mechanism for such a CH_3CN source, but an artificial one was added in a separate run to try to reproduce the MLS observations. Production of ∼0.9–1.7 CH_3CN molecules $cm^{-3}\,s^{-1}$ between 25 and 32 km, and ±5° latitude, with surface and initial boundary conditions unchanged, yields a closer match to the MLS equatorial observations between 25 and 40 km. Both model datasets show more equatorial CH_3CN than MLS below ∼25 km, due to the tropospheric boundary conditions assumed. Above 40 km at the equator, MLS data show greater CH_3CN abundances than either model run.

At 70°N the MLS and model profiles are very different. Both sets of model data show a much faster vertical decrease in mid to upper stratosphere CH_3CN abundances than the MLS data. In both January and July, MLS shows less CH_3CN than either model run below ∼35 km, with higher abundances than the model data above that altitude.

Validity of the MLS detection of a tropical stratospheric peak is clearly dependent on the accuracy of the retrievals showing smaller mixing ratios below the peak. The dominant uncertainty at these levels is spectral contamination from N_2O, whose abundance in the retrievals is taken from

the UARS standard climatology. Tests have shown that the effects of a 50% error in the assumed concentration of N_2O on retrieved equatorial CH_3CN are $<$ 10 pptv at 68 hPa ($\sim$19 km) and $<$ 1 pptv at 46 hPa ($\sim$22 km). Uncertainty in the abundance of other species therefore cannot account for the $\sim$20 pptv magnitude of the observed CH_3CN peak, nor can any known instrumental artifacts.

Figure 3.

Figure 3 compares zonal mean CH_3CN for Dec/Jan and Jun/Jul from MLS and the two model runs discussed. Both MLS and the model show more stratospheric CH_3CN in the tropics than at higher latitudes, as expected for a gas having a tropospheric source and entering the stratosphere through the tropical tropopause. The tropical stratospheric peak is clearly seen in MLS data for both periods. The artificial tropical source in the second model run does not produce a stratospheric peak in the tropics as there is more CH_3CN in the model below $\sim$25 km ($\sim$25 hPa) than in the MLS data; this source has little effect on model results outside the tropics. To further improve the comparison between MLS and the model observations a third model run was performed. In this run, the surface boundary condition was lowered by 25% (this is close to the lower limit of the range of abundances previously observed). The source production was increased to 1.4–5.8 CH_3CN molecules $cm^{-3}\,s^{-1}$, and confined to the equator. The output from this model run, which reproduces the peak in the MLS data is also shown in Figure 3. MLS observations show a broad peak from $\sim$32 hPa to $\sim$10 hPa, while the highest values in the model are confined to the region from $\sim$20 hPa to $\sim$10 hPa.

MLS observes notably less CH_3CN between $\sim$50 and $\sim$5 hPa at high latitudes in winter than in summer; this is not reproduced in the model data, which conversely show greater CH_3CN concentrations in the northern hemisphere than the southern in both January and July, especially below $\sim$30 hPa as seen in Figure 3.

Figure 4.

Figure 5.

Figures 4 and 5 show vertical and horizontal cross sections of MLS CH_3CN (a Kalman smoother has been applied to the MLS data) with model results overlaid as contours. MLS data prior to June 1992 have been omitted because of spectral contamination by SO_2 from the Mt. Pinatubo eruption. The temporal behavior of the tropical peak is interesting. From July to November 1994 CH_3CN abundances in the peak region are depressed. The abundances then steadily increase, reaching a maximum around July 1996. The data show no evidence that this increase is fed from the troposphere. A somewhat similar event is seen from July 1992 to January 1994. The observations seem to indicate a variable stratospheric CH_3CN source in the tropics.

The high latitude panels in Figure 5 show clear annual cycles. These appear more robust in the southern hemisphere than the northern. Qualitatively similar cycles are seen in

the model output. At 70°S and 2.2 hPa, for example, the MLS annual cycle range is ∼4–12 pptv (∼±50%) and the model range is ∼0.07–0.19 pptv (also ∼±50%). The height variation of the annual cycles in both MLS and model seems to indicate descent at high latitudes. It is unclear whether the difference in absolute values between MLS and the model is a manifestation of a source of CH_3CN at lower latitudes. Variations in the tropical to midlatitude stratosphere are less strong and do not show clear cycles.

4. Issues for future study

The MLS observations provide evidence for a previously unknown tropical stratospheric source of CH_3CN at ∼30–10 hPa (∼25–30 km). Ground-based far-infrared measurements at 30°N [*Abbas et al.*, 1987] and microwave observations at 19°N [*Jaramillo et al.*, 1988] have indicated an increase in HCN with altitude between ∼25 and ∼40 km. HCN also has no known stratospheric source. Since there are no identified mechanisms to convert HCN to CH_3CN in the atmosphere, it is speculative to try to link the two phenomena. However, we note that the increase in HCN with altitude in the tropics could be related to that of CH_3CN. Independent observations of both species as a function of altitude in the tropics would be useful. Furthermore, a better understanding of the tropospheric distribution of CH_3CN would better constrain future models, improving their ability to evaluate possible sources in the atmosphere.

Also, a localized CH_3CN enhancement of ∼1000 pptv at 100–68 hPa was seen off the southeast U.S. coast on 25 August 1992, which over several days moved westward and dissipated; the cause of this event is under investigation.

Acknowledgments. The authors thank M.L. Santee for useful comments. The research in this paper done at the Jet Propulsion Laboratory, California Institute of Technology, was under contract with the National Aeronautics and Space Administration. The National Center for Atmospheric Research is sponsored by the National Science Foundation.

References

Abbas, M., et al., Stratosheric distribution of HCN from far infrared observations, *Geophys. Res. Lett.*, *14*, 531–534, 1987.

Arijs, E., and G. Brasseur, Acetonitrile in the stratosphere and implications for positive ion composition, *J. Geophys. Res.*, *91*, 4,003–4,016, 1986.

Becker, K., and A. Ionescu, Acetonitrile in the lower troposphere, *Geophys. Res. Lett.*, *9*, 1,349–1,351, 1982.

Böhringer, H., and F. Arnold, Acetonitrile in the stratosphere – implications from laboratory studies, *Nature*, *290*, 321–322, 1981.

Brasseur, G., et al., Is hydrogen cyanide (HCN) a progenitor of acetonitrile (CH_3CN) in the atmosphere?, *Geophys. Res. Lett.*, *12*, 117–120, 1985.

DeMore, W., et al., Chemical kinetics and photochemical data for use in stratospheric modeling, *Tech. rep.*, Jet Propulsion Laboratory, 1997.

Hamm, S., and P. Warneck, The interhemispheric distribution and the budget of acetonitrile in the troposphere, *J. Geophys. Res.*, *95*, 20,593–20,606, 1990.

Hamm, S., J. Hahn, G. Helas, and P. Warneck, Acetonitrile in the troposphere: Residence time due to rainout and uptake by the ocean, *Geophys. Res. Lett.*, *11*, 1,207–1,210, 1984.

Hamm, S., G. Helas, and P. Warneck, Acetonitrile in the air over Europe, *Geophys. Res. Lett.*, *16*, 483–486, 1989.

Holzinger, R., et al., Biomass burning as a source of formaldehyde, acetaldehyde, methanol, acetone, aceotnitrile and hydrogen cyanide, *Geophys. Res. Lett.*, *26*, 1,161–1,164, 1999.

Jaramillo, M., R. deZafra, J. Barrett, A. Parrish, and P. Solomon, mm-wave observations of stratospheric HCN at tropical latitudes, *Geophys. Res. Lett.*, *15*, 265–268, 1988.

Knop, G., and F. Arnold, Stratospheric trace gas detection using new balloon-borne ACIMS method: Acetonitrile, acetone, and nitric acid, *Geophys. Res. Lett.*, *14*, 1,262–1,265, 1987a.

Knop, G., and F. Arnold, Atmospheric acetonitrile measurements in the tropopause region using aircraft-borne active chemical ionization mass spectrometry, *Planet. Space Sci*, *35*, 259–266, 1987b.

Lobert, J., D. Scharffe, W. Hao, and P. Crutzen, Importance of biomass burning in the atmospheric budgets of nitrogen-containing gasses, *Nature*, *346*, 552–554, 1990.

Murad, E., W. Swider, R. Moss, and S. Toby, Stratospheric sources of CH_3CN and CH_3OH, *Geophys. Res. Lett.*, *11*, 147–150, 1984.

Pickett, H., R. Poynter, and E. Cohen, Submillimeter, millimeter and microwave spectral line catalog, *Tech. rep.*, Jet Propulsion Laboratory, 1992, 80-23, Rev. 3.

Rodgers, C., Characterisation and error analysis of profiles retrieved from remote sounding measurements, *J. Geophys. Res.*, *95*, 5,587–5,595, 1990.

Schneider, J., V. Bürger, and F. Arnold, Methyl cyanide and hydrogen cyanide measurements in the lower stratosphere: Implications for methyl cyanide sources and sinks, *J. Geophys. Res.*, *102*, 25,501–25,506, 1997.

Snider, J., and G. Dawson, Surface acetonitrile near Tucson Arizona, *Geophys. Res. Lett.*, *11*, 241–242, 1984.

Waters, J., et al., Validation of UARS Microwave Limb Sounder ClO measurements, *J. Geophys. Res.*, *101*, 10,091–10,127, 1996.

Waters, J., et al., The UARS and EOS Microwave Limb Sounder (MLS) experiments, *J. Atmos. Sci.*, *56*, 194–217, 1999.

(Received Not yet; revised Not yet;
accepted not yet.)

LIVESEY ET AL.: UARS MLS CH_3CN OBSERVATIONS

LIVESEY ET AL.: UARS MLS CH_3CN OBSERVATIONS

LIVESEY ET AL.: UARS MLS CH_3CN OBSERVATIONS

LIVESEY ET AL.: UARS MLS CH_3CN OBSERVATIONS

LIVESEY ET AL.: UARS MLS CH_3CN OBSERVATIONS

LIVESEY ET AL.: UARS MLS CH_3CN OBSERVATIONS

LIVESEY ET AL.: UARS MLS CH_3CN OBSERVATIONS

LIVESEY ET AL.: UARS MLS CH_3CN OBSERVATIONS

LIVESEY ET AL.: UARS MLS CH_3CN OBSERVATIONS

LIVESEY ET AL.: UARS MLS CH_3CN OBSERVATIONS

Figure Captions

Figure 1. Spectra from MLS bands 2 and 3: zonal mean radiance 10°S–10°N on 8 June 1994. For this region and time the spectra are dominated by CH_3CN emission. Radiances are in units of brightness temperature are averaged over 1/6 of a decade in pressure (∼2.5 km). Intermediate frequency is the difference (both positive and negative) from the 203.267 GHz local oscillator frequency. Emission from $H_2{}^{18}O$ can explain the increase in 100 hPa radiance near 1.5 GHz. The bottom panel shows positions of spectral lines.

Figure 1. Spectra from MLS bands 2 and 3: zonal mean radiance 10°S–10°N on 8 June 1994. For this region and time the spectra are dominated by CH_3CN emission. Radiances are in units of brightness temperature are averaged over 1/6 of a decade in pressure (∼2.5 km). Intermediate frequency is the difference (both positive and negative) from the 203.267 GHz local oscillator frequency. Emission from $H_2{}^{18}O$ can explain the increase in 100 hPa radiance near 1.5 GHz. The bottom panel shows positions of spectral lines.

Figure 2. Comparison of MLS CH_3CN observations with previous observations and output from the SOCRATES model. The MLS profiles shown have been generated from the raw MLS data using a Kalman smoother (see the discussion in Figure 4 caption). The error bars (omitted on the 70°N July profile for clarity) on these profiles indicate the precision of the smoothed estimate (note that for the tropical profile, below ∼30 km, the precision is comparable to the width of the red line). The narrow dashed lines denote output from the standard model run. The heavy dashed lines denote output from the run with an artificial tropical source of stratospheric CH_3CN. The previous observations are reproduced from *Schneider et al.* [1997] (=S 97). Other references are: *Hamm et al.* [1989] (=H 89), and *Knop and Arnold* [1987a/b] (=K+A 87a/b). The balloon and rocket observations shown were all made in central Europe in the late 1970s and early 1980s.

Figure 2. Comparison of MLS CH_3CN observations with previous observations and output from the SOCRATES model. The MLS profiles shown have been generated from the raw MLS data using a Kalman smoother (see the discussion in Figure 4 caption). The error bars (omitted on the 70°N July profile for clarity) on these profiles indicate the precision of the smoothed estimate (note that for the tropical profile, below ∼30 km, the precision is comparable to the width of the red line). The narrow dashed lines denote output from the standard model run. The heavy dashed lines denote output from the run with an artificial tropical source of stratospheric CH_3CN. The previous observations are reproduced from *Schneider et al.* [1997] (=S 97). Other references are: *Hamm et al.* [1989] (=H 89), and *Knop and Arnold* [1987a/b] (=K+A 87a/b). The balloon and rocket observations shown were all made in central Europe in the late 1970s and early 1980s.

Figure 3. MLS CH_3CN zonal mean (a) compared with model results. Model data shown are (b) first model run, (c) run with artificial stratospheric CH_3CN source, (d) run with decreased CH_3CN surface abundance and increased source strength. Model fields are for 1 July year 5 and 1 January year 6 of the runs. The corresponding MLS fields are means of June and July 1993, and December 1992 and January 1993, chosen as they have good data coverage.

Figure 3. MLS CH_3CN zonal mean (a) compared with model results. Model data shown are (b) first model run, (c) run with artificial stratospheric CH_3CN source, (d) run with decreased CH_3CN surface abundance and increased source strength. Model fields are for 1 July year 5 and 1 January year 6 of the runs. The corresponding MLS fields are means of June and July 1993, and December 1992 and January 1993, chosen as they have good data coverage.

Figure 4. Latitude/time cross sections of MLS zonal mean CH_3CN for the period June 1992 to December 1997. The data have been binned into daily zonal means with 10° wide latitude bins centered on the multiples of 10°. This dataset has then been interpolated using a Kalman smoother with a decorrelation rate of 1 pptv/day (yielding a smoothing comparable to a $\sim$5 day running average). There is no interpolation or propagation of information in either the height or latitude dimensions. Paler colors denote regions where, because of data gaps, the estimated precision of the interpolated field is worse than 10 pptv (one contour level). The color levels are as in Figure 3. Overlaid are white contours from the final year of output from the first model run (without the artificial CH_3CN source, see text).

Figure 4. Latitude/time cross sections of MLS zonal mean CH_3CN for the period June 1992 to December 1997. The data have been binned into daily zonal means with 10° wide latitude bins centered on the multiples of 10°. This dataset has then been interpolated using a Kalman smoother with a decorrelation rate of 1 pptv/day (yielding a smoothing comparable to a $\sim$5 day running average). There is no interpolation or propagation of information in either the height or latitude dimensions. Paler colors denote regions where, because of data gaps, the estimated precision of the interpolated field is worse than 10 pptv (one contour level). The color levels are as in Figure 3. Overlaid are white contours from the final year of output from the first model run (without the artificial CH_3CN source, see text).

Figure 5. Height/time cross sections of MLS zonal mean CH_3CN, binned and interpolated as in Figure 4, with overlaid white contours from the model as in Figure 4. Color levels are as in Figure 3. Model contours are logarithmic in the 70°N and 70°S panels and linear elsewhere.

Figure 5. Height/time cross sections of MLS zonal mean CH_3CN, binned and interpolated as in Figure 4, with overlaid white contours from the model as in Figure 4. Color levels are as in Figure 3. Model contours are logarithmic in the 70°N and 70°S panels and linear elsewhere.

Figures

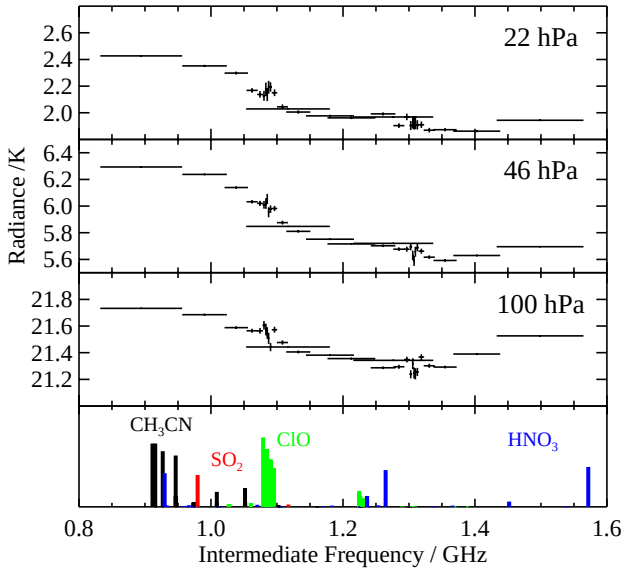

Figure 1. Spectra from MLS bands 2 and 3: zonal mean radiance 10°S–10°N on 8 June 1994. For this region and time the spectra are dominated by CH_3CN emission. Radiances are in units of brightness temperature are averaged over 1/6 of a decade in pressure (∼2.5 km). Intermediate frequency is the difference (both positive and negative) from the 203.267 GHz local oscillator frequency. Emission from $H_2{}^{18}O$ can explain the increase in 100 hPa radiance near 1.5 GHz. The bottom panel shows positions of spectral lines.

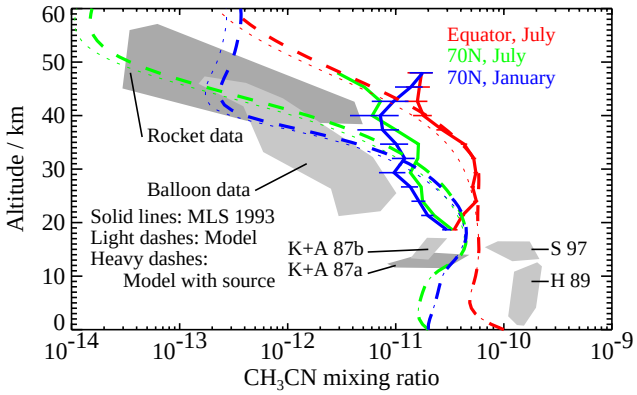

Figure 2. Comparison of MLS CH_3CN observations with previous observations and output from the SOCRATES model. The MLS profiles shown have been generated from the raw MLS data using a Kalman smoother (see the discussion in Figure 4 caption). The error bars (omitted on the 70°N July profile for clarity) on these profiles indicate the precision of the smoothed estimate (note that for the tropical profile, below ∼30 km, the precision is comparable to the width of the red line). The narrow dashed lines denote output from the standard model run. The heavy dashed lines denote output from the run with an artificial tropical source of stratospheric CH_3CN. The previous observations are reproduced from *Schneider et al.* [1997] (=S 97). Other references are: *Hamm et al.* [1989] (=H 89), and *Knop and Arnold* [1987a/b] (=K+A 87a/b). The balloon and rocket observations shown were all made in central Europe in the late 1970s and early 1980s.

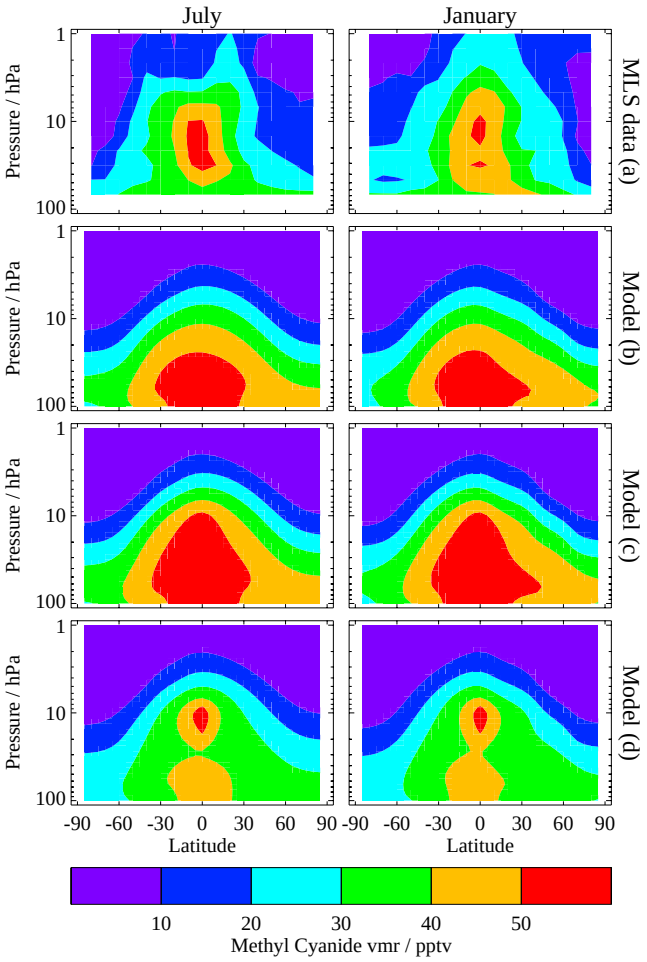

Figure 3. MLS CH_3CN zonal mean (a) compared with model results. Model data shown are (b) first model run, (c) run with artificial stratospheric CH_3CN source, (d) run with decreased CH_3CN surface abundance and increased source strength. Model fields are for 1 July year 5 and 1 January year 6 of the runs. The corresponding MLS fields are means of June and July 1993, and December 1992 and January 1993, chosen as they have good data coverage.

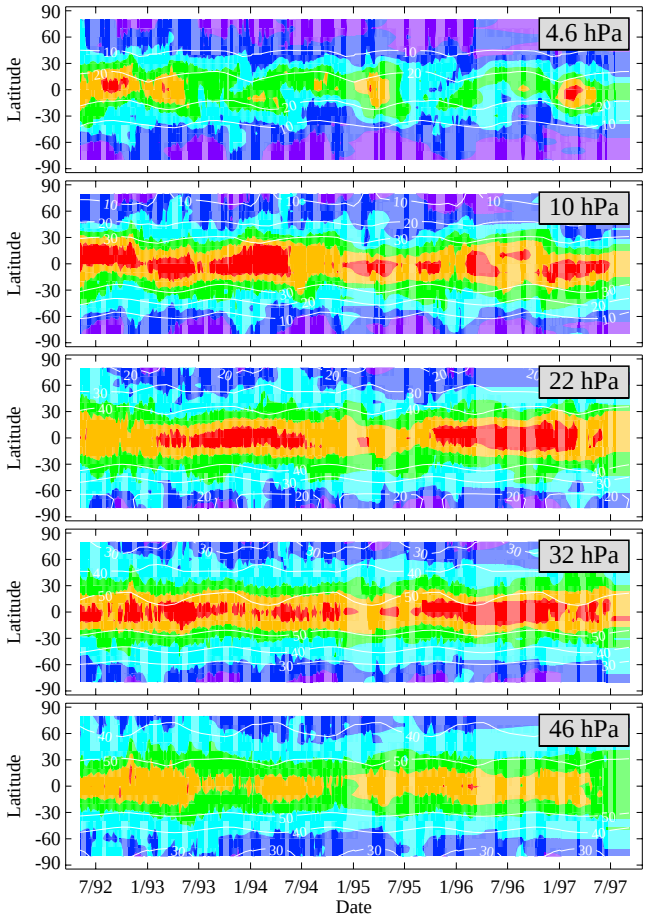

Figure 4. Latitude/time cross sections of MLS zonal mean CH_3CN for the period June 1992 to December 1997. The data have been binned into daily zonal means with 10° wide latitude bins centered on the multiples of 10°. This dataset has then been interpolated using a Kalman smoother with a decorrelation rate of 1 pptv/day (yielding a smoothing comparable to a ∼5 day running average). There is no interpolation or propagation of information in either the height or latitude dimensions. Paler colors denote regions where, because of data gaps, the estimated precision of the interpolated field is worse than 10 pptv (one contour level). The color levels are as in Figure 3. Overlaid are white contours from the final year of output from the first model run (without the artificial CH_3CN source, see text).

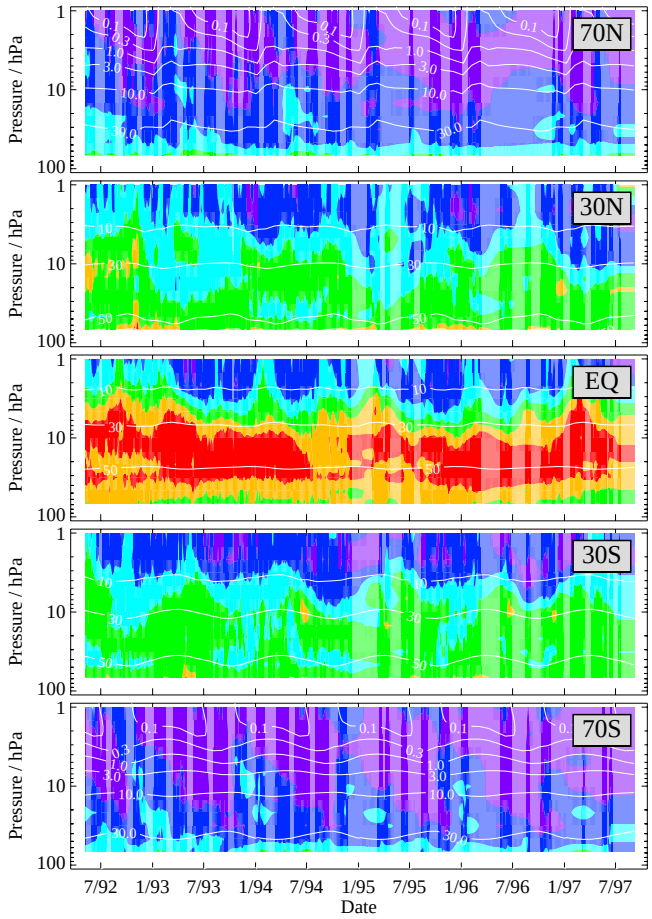

Figure 5. Height/time cross sections of MLS zonal mean CH_3CN, binned and interpolated as in Figure 4, with overlaid white contours from the model as in Figure 4. Color levels are as in Figure 3. Model contours are logarithmic in the 70°N and 70°S panels and linear elsewhere.

CH_3CN in the stratosphere has been measured by the Microwave Limb Sounder (MLS) on the Upper Atmosphere Research Satellite (UARS), providing the first global CH_3CN dataset. The MLS observations are in broad agreement with past high and midlatitude observations of CH_3CN, although concentrations are a little larger than previously observed. In the tropics, where CH_3CN has not up to now been measured, a persistent 'peak' in the profiles is seen around 22 hPa, indicating a possible stratospheric source. Comparisons are made with the NCAR SOCRATES model, including runs having an artificial tropical stratospheric CH_3CN source.